

1 **Taphonomic damage obfuscates interpretation of the retroarticular region of the *Asteriornis***

2 **mandible**

3

4 Abi Crane<sup>1\*</sup>, Juan Benito<sup>1</sup>, Albert Chen<sup>1</sup>, Grace Musser<sup>2</sup>, Christopher R. Torres<sup>3,4</sup>, Julia A. Clarke<sup>4</sup>,

5 Stephan Lautenschlager<sup>5</sup>, Daniel T. Ksepka<sup>6</sup>, Daniel J. Field<sup>1,7\*</sup>

6

7 <sup>1</sup>Department of Earth Sciences, University of Cambridge

8 <sup>2</sup>The Smithsonian National Museum of Natural History, Washington, DC

9 <sup>3</sup>Heritage College of Osteopathic Medicine, Ohio University

10 <sup>4</sup>Jackson School of Geosciences, University of Texas at Austin

11 <sup>5</sup>University of Birmingham

12 <sup>6</sup>Bruce Museum, Greenwich, Connecticut

13 <sup>7</sup>Museum of Zoology, University of Cambridge

14 \*Authors for correspondence: ac2219@cam.ac.uk; djf70@cam.ac.uk

15

16

17

18

19

20

21

22

23    **Abstract**

24    *Asteriornis maastrichtensis*, from the latest Cretaceous of Belgium, is among the oldest known crown  
25    bird fossils, and its three-dimensionally preserved skull provides the most substantial insights into the  
26    cranial morphology of early crown birds to date. Phylogenetic analyses recovered *Asteriornis* as a  
27    total-group member of Galloanserae (the clade uniting Galliformes and Anseriformes. One important  
28    feature supporting this placement was enlargement of the retroarticular processes, which form  
29    elongate caudal extensions of the mandible in extant Galloanserae. Here, we reinterpret the jaw of  
30    *Asteriornis* and illustrate that the caudalmost portion of the mandibles are in fact not preserved.  
31    Instead, the caudal extremities of both the left and right mandibular rami extend to the surface of the  
32    fossil block containing the holotype skull, where they have eroded away. The originally identified  
33    retroarticular process of the right mandible—which exhibits a morphology and orientation strikingly  
34    similar to the retroarticular processes of certain extant and fossil galloanserans, including the early  
35    Palaeogene total-clade anseriforms *Conflictio* and *Nettapterornis*—instead represents a twisted and  
36    caudally displaced medial process. Nonetheless, anatomical comparisons with extant taxa reveal that  
37    we are unable to exclude the possibility that *Asteriornis* exhibited robust retroarticular processes  
38    comparable to those of extant Galloanserae. In light of the reinterpreted morphology of the *Asteriornis*  
39    mandible, we update the original anatomical character matrix used to investigate its phylogenetic  
40    relationships, and our revised phylogenetic analyses continue to support its position as a total-group  
41    galloanseran, as initially interpreted. We demonstrate additional morphological traits of the mandible  
42    supporting this phylogenetic position and provide new data on the nature and distribution of  
43    retroarticular processes among early crown birds.

44

45

46

47

48

49 **Introduction**

50 *Asteriornis maastrichtensis* is one of only two well-represented Mesozoic taxa that have been  
51 confidently identified as members of Neornithes (crown group birds) (Clarke et al., 2005; Clarke et  
52 al., 2016; Field et al., 2020a; Mayr, 2022a), the sole clade of birds to survive the end-Cretaceous mass  
53 extinction (Longrich et al., 2011). The holotype and only known specimen, from the latest Cretaceous  
54 Belgium, consists of fragmentary post-cranial material and a nearly complete, three-dimensionally  
55 preserved skull (Field et al., 2020a). On the basis of phylogenetic analyses, *Asteriornis* was initially  
56 interpreted as a total-group galloanseran, exhibiting a unique combination of typically galliform and  
57 anseriform features suggesting a phylogenetic position close to the most recent common ancestor of  
58 Galliformes and Anseriformes. However, subsequent analyses including *Asteriornis* have instead  
59 recovered it as a stem-palaeognath (Torres et al., 2021; Musser and Clarke 2022), a member of the  
60 sister clade to the remainder of the avian crown group, and a notable result as it would constitute the  
61 only known representative of a Mesozoic total-clade palaeognath (Widrig et al. 2022), filling a major  
62 gap in the crown bird fossil record (Field et al. 2020b). The phylogenetic placement of *Asteriornis* has  
63 implications for interpreting the ancestral condition of crown group birds, and for informing  
64 divergence-time estimates for some of the deepest extant clades within the avian crown group. As  
65 such, a more complete and accurate understanding of the morphology and phylogenetic position of  
66 *Asteriornis* may provide important insight into the earliest stages of neornithine evolution.

67 Galliformes (landfowl) and Anseriformes (waterfowl) are now well understood to be sister  
68 groups occupying a position sister to the major extant clade Neoaves (Sibley & Ahlquist, 1990;  
69 Livezey, 1997; Mayr & Clarke, 2003; Ericson et al., 2006; Hackett et al., 2008; Mayr, 2008; Jarvis et  
70 al., 2014; Prum et al., 2015; Reddy et al., 2017; Kimball et al., 2019; Kuhl et al., 2021), but this  
71 relationship remained controversial prior to the widespread adoption of molecular phylogenetics  
72 (Olson & Feduccia, 1980; Ericson, 1996, 1997). First suggested as early as the 19<sup>th</sup> century (Garrod,  
73 1873), the clade Galloanserae (defined as the most recent common ancestor of Galliformes and  
74 Anseriformes, and all of its descendants (Mindell, 2020)) has hitherto only been supported by a  
75 limited number of morphological synapomorphies (Cracraft & Mindell, 1989; Ericson, 1996). Other

76 previously proposed phylogenetic arrangements included Anseriformes as sister to the neoavian  
77 clades Charadriiformes (Olson & Feduccia, 1980; Feduccia, 1999) and ‘Ciconiiformes’ (Ericson,  
78 1996), now recognised as a polyphyletic assemblage including storks, herons, ibises and flamingos  
79 (Ericson et al., 2006; Hackett et al., 2008; Jarvis et al., 2014; Kuramoto et al., 2015; Prum et al., 2015;  
80 Reddy et al., 2017; Kuhl et al., 2021), with Galliformes sometimes instead hypothesised to form a  
81 clade with Palaeognathae (Feduccia, 1999; Bourdon et al., 2010). Although the monophyly of crown  
82 Galloanserae is no longer controversial, the scarcity of osteological synapomorphies diagnosing the  
83 clade imposes challenges for identifying representatives of total-group Galloanserae in the fossil  
84 record.

85 The few osteological synapomorphies diagnosing Galloanserae are largely restricted to the  
86 skull (Ericson, 1996; Cracraft et al., 2001; Mayr, 2008; Bourdon et al., 2010; Mayr, 2011; Field et al.,  
87 2020a; Musser and Clarke 2022). Among these, the distinctive morphology of the pterygoid and the  
88 bicondylar quadrate-mandible articulation (Cracraft & Mindell, 1989; Ericson, 1996) have come  
89 under recent scrutiny, with analyses suggesting that they may instead represent retained  
90 symplesiomorphies of Neornithes rather than synapomorphies of Galloanserae (Mayr et al., 2018;  
91 Tambussi et al., 2019; Field et al., 2020a; Benito et al., 2022a). By contrast, the expanded, caudally  
92 projecting retroarticular process (which was considered convergent between galliforms and  
93 anseriforms in earlier work arguing against the monophyly of Galloanserae (Olson & Feduccia, 1980;  
94 Ericson, 1996, 1997; Olson, 1999), now stands as one of the few uncontroversial osteological  
95 synapomorphies of crown Galloanserae (Mayr, 2016; Field et al., 2020a), and this structure has  
96 played an important role in substantiating the assignment of several fossil birds to Galloanserae,  
97 including *Presbyornis* (Ericson, 1997; Livezey, 1997) and *Nettapterornis* (formerly *Anatalavis*  
98 *oxfordi*; Olson, 1999). Conversely, the apparent absence of enlarged, caudally projecting retroarticular  
99 processes has also been used to dispute putative galloanseran affinities for controversial fossil bird  
100 taxa, such as *Vegavis* (Mayr et al., 2018).

101 The retroarticular process is a caudally projecting process of the mandible extending caudal to  
102 the quadrate-mandible articulation, and its architecture typically comprises an extension of the angular

103 bone within the mandibular postdentary complex (Baumel & Witmer, 1993; Vanden Berge & Zweers,  
104 1993; Ericson, 1997). The retroarticular process acts as an area of insertion for the M. depressor  
105 mandibulae, and their size and shape are often correlated (Bock, 1964; Zusi, 1967; Ericson, 1997).  
106 The retroarticular therefore plays an important functional role in the movement of the mandible,  
107 especially with respect to gaping and prying behaviour (Beecher, 1951; Zusi, 1967; Zweers & Berge,  
108 1996; Previatto, 2012). Long retroarticular processes have been interpreted as adaptations for  
109 ecologies necessitating the beak to be opened against resistance (e.g., filter feeders; Bock, 1964; Zusi,  
110 1967), or requiring a wide or forceful gape, as in some frugivorous or granivorous birds (Mayr, 2013).  
111 Among extant birds, well-developed retroarticular processes are uniformly present among  
112 representatives of Galloanserae, and are found in several neoavian taxa, including flamingos  
113 (Phoenicopteridae) and some representatives of Charadriiformes, Bucerotiformes, and Passeriformes  
114 (Beecher, 1951; Baumel & Witmer, 1993; Ericson, 1996; Zweers & Berge, 1996; Ericson, 1997;  
115 Mayr, 2005; Mayr et al., 2018; Field et al., 2020a; Mayr, 2022b). The morphology of the retroarticular  
116 process shows considerable variation among extant birds; the shape of the process ranges from being  
117 mediolaterally compressed and dorsoventrally deep in ducks (Anatidae) and flamingos, to a more  
118 rounded and mediolaterally wide form in landfowl (Galliformes) and screamers (Anhimidae)  
119 (Ericson, 1997).

120 Field et al. (2020a) interpreted *Asteriornis maastrichtensis* as possessing large and hooked  
121 retroarticular processes in their original description. The morphology of the *Asteriornis* retroarticular  
122 was considered comparable to that of the pan-anseriform *Nettapterornis oxfordi* (Olson, 1999), and  
123 was included as part of a suite of characters supporting galloanseran affinities for *Asteriornis* (Field et  
124 al. 2020a Fig. 1d). However, restudy of the CT data by Torres et al. (2021) resulted in a different  
125 interpretation, identifying the ‘retroarticular process’ of *Asteriornis* as a caudally displaced medial  
126 process of the mandible, twisted into a dorsoventral orientation. Further evaluation of high-contrast  
127 surface meshes confirms this observation and provides additional insight into the anatomy of the  
128 *Asteriornis* mandible. In its preserved position the process exhibits a dorsally directed hook and  
129 projects from the caudal extremity of the mandible, strongly resembling the retroarticular morphology

130 of many anseriforms. Indeed, the overall shape of the retroarticular and medial processes in certain  
131 pan-galloanserans can be remarkably similar, as in the pan-anseriform *Conflictto* (Tambussi et al.,  
132 2019). When retrodeformed, however, this process shows a clear, although not exact, symmetry with  
133 the medial process of the left mandibular ramus.

134 Reinvestigation of the unprepared holotype of *Asteriornis* reveals that the caudal extremities  
135 of both the lower jaws eroded away at the surface of the fossil block (Fig. 4). We therefore sought to  
136 evaluate whether the state of preservation of the holotype mandibles could enable us to exclude the  
137 possibility that a galloanseran-like retroarticular was present in *Asteriornis*, which might have  
138 important implications for assessing the phylogenetic position of this crucial early neornithine, and  
139 could bear on our understanding of the evolutionary history of a key galloanseran synapomorphy. To  
140 assess the possibility of a retroarticular process having originally been present in *Asteriornis*, we  
141 compared the observable anatomy of the caudal ends of the preserved mandibles of *Asteriornis* with  
142 those of a range of extant bird taxa with their retroarticular processes intact and digitally removed. We  
143 also updated the phylogenetic matrix used by Field et al. (2020a) in light of our observations to assess  
144 their potential impact on the inferred phylogenetic position of *Asteriornis*.

145

## 146 **Methods**

### 147 *Anatomical Comparisons*

#### 148 *Taxon selection*

149 Our sample included osteologically mature representatives of ten extant taxa. Six galloanserans were  
150 chosen to represent the spectrum of retroarticular morphologies represented within the clade. In this  
151 sample, retroarticular morphologies range from the mediolaterally narrow, ‘blade-like’ retroarticular  
152 diagnostic of Anseres (anseriforms other than Anhimidae) to the mediolaterally thicker processes  
153 typical of galliforms, which are more rounded in transverse section. We also included an aberrant  
154 specimen of *Meleagris gallopavo* with extremely elongated retroarticular processes atypical even for  
155 domestic members of this species in order to maximise the range of galloanseran retroarticular

156 morphologies encompassed by our sample. Several non-galloanseran taxa were sampled for  
157 comparative purposes including two representatives of Palaeognathae (recovered as the closest extant  
158 relatives of *Asteriornis* by Torres et al. 2021) and two members of Neoaves: the flamingo  
159 *Phoenicopterus roseus*, which exhibits a large retroarticular process that may be convergently similar  
160 to that of anseriforms, and the shearwater *Puffinus puffinus*, which lacks a retroarticular process.

161 *Imaging*

162 All specimens were scanned using high-resolution computed tomography (CT); scanning was  
163 performed at the Cambridge Biotomography Centre (CBC) using a Nikon 49 Metrology XT H 225 ST  
164 high-resolution CT scanner. Scanned specimens were digitally segmented and rendered in  
165 VGSTUDIO MAX 3.4 (Volume Graphics, Heidelberg, Germany). In order to make anatomical  
166 comparisons between the broken caudal ends of the *Asteriornis* mandible and extant taxa, the caudal  
167 portions of the mandibles of the modern specimens (the ‘retroarticular regions’) were digitally  
168 removed. The retroarticular region was defined as including anything positioned caudal to the caudal  
169 end of the base of the medial process; this approximates the region of missing material from the  
170 mandibular rami of the *Asteriornis* holotype. This region was digitally removed using the clipping  
171 plane tool in VGSTUDIO MAX, and images were taken with and without the presence of this  
172 retroarticular region.

173 Due to an error during the original CT scanning process, the CT-data of *Asteriornis* studied  
174 by Field et al. (2020a) were left-right mirrored with respect to the actual fossil material; the scans  
175 used in the current work are corrected in reference to the original fossil. Features described as  
176 pertaining to the ‘left’ mandible by Field et al. (2020a) are therefore referred to as ‘right’ here, and  
177 vice versa.

178

179 *Phylogenetic analysis*

180 We reanalysed the phylogenetic position of *Asteriornis* using a morphological dataset modified from  
181 Field et al. (2020a). We added one taxon to this dataset, the recently described putative stem-

182 anseriform *Anachronornis*, based on scoring by Houde et al. (2023). For *Asteriornis*, we rescored  
183 characters 64 and 292 (Retroarticular process, shape), and 291 (Retroarticular process, presence) to  
184 unknown (see Results and Discussion). Additionally, we updated the scorings of *Vegavis* based on a  
185 recent redescription of the holotype by Acosta Hospitaleche and Worthy (2021). Finally, we rescored  
186 crown galliforms as having two sternal incisures (character 87) following comments on the homology  
187 of avian sternal trabeculae by Livezey and Zusi (2006), and rescored characters 271 and 272 as  
188 inapplicable for taxa lacking a hallux. The updated dataset consisting of 40 taxa and 297 characters  
189 was analysed under both maximum parsimony and Bayesian phylogenetic optimality criteria with  
190 molecular scaffolds derived from previous studies (Hackett et al., 2008; Gonzalez et al., 2009; Harris  
191 et al., 2014; Jarvis et al., 2014; Prum et al., 2015; Reddy et al., 2017; Kimball et al., 2019; Kimball et  
192 al., 2021; Kuhl et al., 2021; Simmons et al., 2022).

193 Maximum parsimony analyses were conducted in TNT v.1.5 (Goloboff & Catalano, 2016).  
194 After increasing the maximum number of trees to 99,999, a new technology search was run in which a  
195 minimum length tree was found in 10 replicates and default parameters were set for sectorial search,  
196 ratchet, tree drift, and tree fusion. After this, the maximum number of trees was set to 100 and a  
197 traditional search with default parameters was run on the trees in RAM to explore treespace more  
198 extensively. Absolute bootstrap frequencies were obtained from 1,000 replicates under a traditional  
199 search with default parameters.

200 Undated and tip-dated Bayesian phylogenetic analyses were conducted in MrBayes 3.2.7a  
201 (Ronquist et al., 2012) using the CIPRES Science Gateway (Miller et al., 2010), with tip-dating run  
202 under the fossilized birth-death model (Zhang et al., 2016). Priors and parameters followed those used  
203 by Field et al. (2020a), except as stated below. Age priors for extinct taxa were changed to uniform  
204 prior distributions spanning the age range of fossil occurrences, following recent work highlighting  
205 the importance of incorporating stratigraphic uncertainty into tip-dating analyses (Barido-Sottani et  
206 al., 2019; Püschel et al., 2020). Age ranges were based on previous literature (Benton & Donoghue,  
207 Mayr & Rubilar-Rogers, 2010; Ksepka & Clarke, 2015; Collinson et al., 2016; Worthy et al.,  
208 2017; Tambussi et al., 2019; Mayr et al., 2021; Houde et al., 2023), with updated ages for *Asteriornis*

209 and *Vegavis* following recent stratigraphic studies of the Maastricht Formation and the Lopez de  
210 Bertodano Formation, respectively (Vellekoop et al., 2022; Roberts et al., 2023). Morphological  
211 synapomorphies were optimized under parsimony onto resulting tree topologies using TNT.

212

## 213 **Results and Discussion**

### 214 ***The retroarticular region of *Asteriornis****

215 The mandible of *Asteriornis* is taphonomically fragmented and the caudal ends of the mandibular  
216 rami are exposed at the surface of the block of the *Asteriornis* holotype (Fig. 1). The fossil is broken  
217 along a plane which has resulted in the loss of the caudal portion of the skull, including the occipital  
218 region, and the caudal extremities of the mandibles (Fig. 2a). The rostral and medial surfaces of the  
219 right articular region (Fig. 2c) are more completely preserved than the equivalent region of the left  
220 ramus, although this region of the mandible, including the medial process, has been taphonomically  
221 twisted, such that the long axis of the medial process is oriented dorsoventrally rather than  
222 mediolaterally. The tip of the medial process is well-preserved, showing a rostrally deflected tip,  
223 initially mistaken for a dorsally hooked tip as seen in the retroarticular processes of many anseriforms  
224 (Field et al. 2020a). The retroarticular process in the sampled extant taxa extends from the articular  
225 region on the caudal surface of the mandible in line with the long axis of the mandibular ramus (Fig.  
226 3). Given the preservation of the right mandible of *Asteriornis*, it is clear that the region of the  
227 mandible that would have supported a retroarticular process, if one was present, is completely missing  
228 (Fig. 2c). The caudal portion of the right mandibular ramus is thus far too incomplete to exclude the  
229 possibility of a retroarticular process having originally been present.

230 The left articular region is more fragmentary than the right articular region along its medial  
231 and rostral surfaces, yet is more complete than the right articular region along its lateral and caudal  
232 surfaces (Fig. 2b). The lateral process of the mandible is visible as a rostrocaudally elongate and  
233 mediolaterally shallow ridge extending along the lateral surface of the articular region. The caudal end  
234 of this process curves sharply towards the rostrocaudal midline of the mandibular ramus. Similarly,

235 the caudal surface of the tip of the medial process appears to be preserved, and angles caudolaterally  
236 towards the middle of the mandibular ramus. The region between these two preserved caudal surfaces  
237 is broken, exposing the interior of the bone as an approximately triangular cross-section. The deepest  
238 part of this broken region is situated at the point where the break contacts the midline of the ramus  
239 towards the ventral surface, with the most caudally positioned intact portion of the mandible being the  
240 lateral process. As such, it appears that the original presence of a retroarticular process on the left  
241 mandibular ramus cannot be excluded either.

242

243 *Comparisons with extant taxa*

244 The more complete caudal region of the left ramus of *Asteriornis* was compared with those of a range  
245 of extant taxa in order to determine whether the potential presence or absence of a retroarticular  
246 process in *Asteriornis* could be assessed (Fig. 3). The retroarticular processes of the surveyed taxa  
247 were digitally removed in order to approximate the preservation of this region in the *Asteriornis*  
248 holotype (Fig. 4). Given that the retroarticular process in extant taxa extends from the caudal surface  
249 in line with the long axis of the mandibular ramus (Fig. 3), comparisons with extant taxa illustrate that  
250 the preserved portions of the caudal surface of the articular region in *Asteriornis* do not include the  
251 region from which a potential retroarticular would extend (Fig. 4a), precluding any confident  
252 assessment of the original presence or absence of galloanseran-like retroarticular processes in  
253 *Asteriornis*.

254

255 *Implications for the phylogenetic position of Asteriornis*

256 In the absence of evidence for enlarged retroarticular processes—an important galloanseran  
257 synapomorphy—the phylogenetic position of *Asteriornis* is in need of re-evaluation. Torres et al.  
258 (2021) reconstructed the mandible of *Asteriornis* with the medial process correctly positioned and  
259 identified in their supplementary information, although this was not discussed in that study. Their  
260 phylogenetic analysis found *Asteriornis* as a stem-palaeognath, albeit with weak statistical support. As

261 such, the interpretation of *Asteriornis* as a stem-palaeognath was not emphasised in that study and was  
262 ascribed to a dearth of phylogenetically informative characters. The dataset used by Torres et al.  
263 (2021), an updated version of datasets used in Clarke (2004), Clarke et al. (2006), Huang et al. (2016),  
264 and Field et al. (2018) (though see Benito et al. (2022b) for critiques of this dataset), was primarily  
265 aimed at resolving stem-bird phylogeny with limited power to resolve neornithine phylogeny. Indeed,  
266 those authors reported that constraining *Asteriornis* to be a member of total-group Galloanserae in  
267 their analyses extended the length of their most parsimonious trees by only a single step. Moreover,  
268 no characters related to either the presence or morphology of the retroarticular process were included  
269 in the phylogenetic character matrix used in that study; thus, their reinterpretation of the originally  
270 identified retroarticular process of *Asteriornis* had no influence on its inferred phylogenetic position.  
271 Using an updated version of the same matrix, Benito et al. (2022a) found *Asteriornis* to be variably  
272 positioned as a stem-palaeognath under maximum parsimony, and as a crown anseriform under  
273 Bayesian inference, though the latter position is considered to be highly unlikely.

274 Musser and Clarke (2022) included *Asteriornis* in their new dataset for Galloanserae that  
275 includes more extant and extinct galloanserans than any previous dataset, with a particular focus on  
276 Anseriformes. *Asteriornis* was inferred as a stem-palaeognath in two analyses of that dataset: an  
277 analysis of morphological data under parsimony, and a Bayesian analysis of combined molecular and  
278 morphological data. However, that dataset contains a limited sample of palaeognaths, including only a  
279 tinamou and several lithornithids. In morphology-only analyses including the fossil anseriform *Wilaru*  
280 *tedfordi*, *Asteriornis* was inferred as a stem palaeognath with high bootstrap support. However, when  
281 *Wilaru* was excluded from their morphological analysis, *Asteriornis* was inferred as the sister taxon to  
282 Galloanserae with low support. Within both Bayesian analyses using combined data, *Asteriornis* was  
283 again recovered as a stem-palaeognath with low support.

284 Using the newly updated version of the Field et al. (2020a) dataset in which the presence and  
285 shape of the retroarticular were scored as unknown in *Asteriornis*, our maximum parsimony analysis  
286 recovered three most parsimonious trees (MPTs) with a consistency index (CI) of 0.255 and a  
287 retention index (RI) of 0.592. The strict consensus of all MPTs placed *Asteriornis* as a stem-galliform

288 of unresolved affinities with respect to the Eocene taxon *Gallinuloides*, contrasting with the  
289 placement of *Asteroornis* on the galloanseran stem by the maximum parsimony analysis of Field et al.  
290 (2020a). As in Field et al. (2020a), statistical support for most deep divergences within the phylogeny  
291 was weak, with the clade uniting *Asteroornis*, *Gallinuloides*, and crown galliforms having a bootstrap  
292 support value of 26% and a Bremer support value of 2, likely due to the unstable positions of fossil  
293 taxa in the dataset. Bayesian analyses of the updated dataset were consistent with those of Field et al.  
294 (2020a) in recovering *Asteroornis* as stemward of *Gallinuloides* in tip-dating analysis, and as a stem-  
295 galliform crownward of *Gallinuloides* in undated analysis. Statistical support for placing *Asteroornis*  
296 crownward of *Gallinuloides* was low, with a posterior probability (PP) of 0.57, but support for an  
297 exclusive clade uniting *Asteroornis*, *Gallinuloides*, and crown galliforms was high (PP = 1 in undated  
298 analysis and 0.96 under tip-dating). These results support the initial interpretation of *Asteroornis* as a  
299 member of total-group Galloanserae, and potentially a member of total-group Galliformes (Field et  
300 al., 2020a).

301 Field et al. (2020a) reported that no retroarticular traits were inferred as synapomorphies of  
302 the *Asteroornis* + Galloanserae clade under maximum parsimony; as such, it is unlikely that the  
303 rescore of characters related to the presence and morphology of the retroarticular process had a  
304 major effect on the inferred phylogenetic position of *Asteroornis* in that study. Therefore, the shift in  
305 the position of *Asteroornis* under maximum parsimony, from stem-galloanseran to stem-galliform,  
306 might instead be related to rescore of *Vegavis* and adding *Anachronornis*. Notably, the maximum  
307 parsimony and tip-dated Bayesian topologies we recovered were identical to those found by Houde et  
308 al. (2023), who also applied both of these changes to the Field et al. (2020a) dataset. As a further test  
309 of this hypothesis, we ran additional maximum parsimony analyses of our dataset in which scores for  
310 all retroarticular characters were reverted to those originally used by Field et al. (2020a). The resulting  
311 trees remained topologically unchanged from the results of our primary parsimony analysis (see  
312 Supplementary Material).

313 Although the presence of a retroarticular process cannot be confirmed in *Asteroornis*,  
314 additional characters support its placement as a total-group galloanseran and more broadly as a

315 neognath. Under all of our recovered topologies, the presence of a rostromedial foramen in the otic  
316 process of the quadrate was optimized as a synapomorphy uniting *Asteriornis* with crown-group  
317 galliforms. This trait has also been documented in some other neognathous birds, including *Conficto*  
318 and a few extant anseriforms, but not in palaeognaths (Tambussi et al., 2019; Field et al., 2020a).  
319 *Asteriornis* additionally exhibits long, dorsally oriented medial processes of the mandible and a  
320 frontal depression forming a shallow, elongate groove, which are identified as synapomorphies of  
321 Galloanserae under some of our tree topologies. Furthermore, the presence of a subcapitular tubercle  
322 on the quadrate is widely found in Neognathae (Elzanowski & Stidham, 2010, 2011; Field et al.,  
323 2020a), and is supported as a potential synapomorphy of this clade by our analyses. Finally, we  
324 inferred two femoral characters observable in *Asteriornis* as possible synapomorphies of Neognathae:  
325 a caudally prominent medial supracondylar crest that interrupts the internal margin of the distal  
326 femoral shaft, as well as a poorly defined impression for the cranial cruciate ligament. These femoral  
327 characters are not found in any of the palaeognathous taxa sampled in our dataset, including  
328 Lithornithidae, a group of putative stem palaeognaths from the Paleogene. See Supplementary  
329 Material for further details of inferred synapomorphies from our analyses.

330 For comparison, we ran another maximum parsimony analysis in which *Asteriornis* was  
331 constrained to be a member of total-group Palaeognathae. Enforcing this constraint resulted in the  
332 recovery of two MPTs that were five steps longer than those found by our primary parsimony  
333 analysis. *Asteriornis* was recovered as the most stemward stem-palaeognath, whereas lithornithids  
334 were variably recovered as more crownward stem-palaeognaths or the sister group to *Tinamus*. Only a  
335 single unambiguous synapomorphy could be optimized in support for the clade uniting *Asteriornis*  
336 with crown palaeognaths: a splenial unfused to the dentary in adults, a character notably also present  
337 in extant megapodes (Galliformes: Megapodiidae). Of note, however, is the fact that the absolute age  
338 of *Asteriornis* at death remains unknown; thus, whether the unfused splenial of *Asteriornis* would  
339 have persisted in fully osteologically mature individuals cannot be unambiguously assessed. Overall,  
340 the results of our quantitative phylogenetic analyses and anatomical observations all suggest that a

341 position within total-group Galloanserae is the best supported hypothesis for the affinities of  
342 *Asteriornis*, irrespective of our reinterpretation of its caudal mandibular anatomy.

343

344 ***Morphology of the retroarticular region in crown birds***

345 *Galloanserae*

346 The preserved caudal portion of the mandible of *Asteriornis* bears close resemblance to that of some  
347 galloanseran taxa after their retroarticular processes were digitally removed. Most notable are  
348 morphological similarities to the mandibles of the megapodes *Alectura lathami* and *Leipoa ocellata*  
349 (Fig. 4e,f), and the anhimid *Chauna torquata* (Fig. 4b), such as the shape and proportions of the  
350 lateral and medial processes. The lateral process of *Asteriornis* is most similar to that of *Alectura* and  
351 *Leipoa*, being relatively mediolaterally shallow and rostrocaudally long. The prominent medial  
352 process of *Asteriornis* is triangular in dorsal view and is similar in shape to that of *Chauna* and  
353 galliforms, whereas it is rostrocaudally narrower in anatids. Its moderate dorsal deflection in  
354 *Asteriornis* matches the condition in *Alectura*, *Leipoa* and *Chauna*, in contrast to the more steeply  
355 dorsally-pointed medial processes of anatids and other galliforms. Additionally, a sharp and  
356 prominent ridge along the ventral surface of the articular region in *Asteriornis*, in line with the long  
357 axis of the mandibular ramus, is similar to the condition in *Chauna*, but is developed to a lesser extent  
358 in *Alectura* and *Leipoa*. Importantly, Megapodiidae and Anhimidae represent the extant sister taxa to  
359 the rest of Galliformes and Anseriformes, respectively (Ericson, 1997; Livezey, 1997; Cracraft, 2001).  
360 Indeed, recent work suggests that other aspects of the jaw apparatus of megapodes and anhimids,  
361 namely the three-dimensional geometry of the quadrate, bear striking similarities to the inferred  
362 plesiomorphic condition of galloanserans (Kuo et al., 2023), corroborating earlier qualitative  
363 hypotheses (Elzanowski & Stidham, 2011; Elzanowski & Boles, 2012; Houde et al., 2023). The  
364 striking similarities between the preserved portions of the caudal mandible of *Asteriornis* and those of  
365 megapodes and anhimids is therefore in line with the hypothesis that *Asteriornis* may represent either

366 a crownward stem galloanseran, or an early stem-galliform or stem-anseriform, as originally  
367 hypothesised by Field et al. (2020a).

368           Similarly, this region of the mandible of *Asteriornis* is similar to that of several fossil total-  
369 group galloanserans. Most notable is the resemblance to the caudal part of the mandible of the  
370 hypothesised early stem-anseriform *Conflictto* (Tambussi et al., 2019; Field et al., 2020a). The medial  
371 process is similarly proportioned in both taxa, and both show a slight rostral curvature at the tip,  
372 which is preserved most clearly on the right ramus of *Asteriornis*. The lateral process is also of similar  
373 size and shape in both taxa, presenting as a mediolaterally shallow, rostrocaudally oriented ridge  
374 along the lateral surface of the articular region. The prominence of the lateral processes and depth of  
375 the articular regions of the hypothesised total-group anseriforms *Nettapterornis*, *Anachronornis* and  
376 *Danielsavis* are also reminiscent of the condition in *Asteriornis* (Olson, 1999; Houde et al., 2023); the  
377 latter two taxa additionally exhibit a medial process with a shallowly dorsal orientation and a rostrally  
378 hooked tip similar to that of both *Conflictto* and *Asteriornis* (Houde et al., 2023). The morphological  
379 similarities in this region of the mandible of *Asteriornis* with those of fossil pan-anseriforms further  
380 support the interpretation of *Asteriornis* as a total-group galloanseran near the origin of the crown  
381 group.

382           By contrast, the caudal parts of the mandible of *Asteriornis* are markedly dissimilar to those  
383 of Anatidae, which also exhibit strikingly derived quadrates (Kuo et al. 2023). The anatids surveyed  
384 (*Anas platyrhynchos* and *Mergus albellus*; Fig. 4c,d) show a highly derived mandibular morphology  
385 including a large and deep depression (Ericson, 1997; Olson, 1999) between the mandibular ramus  
386 and the medial process, extending along the caudal surface of the latter, known as the recessus  
387 conicalis. The recessus conicalis is clearly exposed and visible upon removal of the retroarticular  
388 process in these taxa, and results in a distinctive morphology towards the rostral end of the articular  
389 region as the articular comprises part of this deep, caudally positioned depression (Fig. 4c,d). The  
390 regions of the caudal part of the mandible of *Asteriornis* which are preserved, including the medial  
391 process, clearly exclude the presence of a similarly deep, anatid-like recessus conicalis. The absence  
392 of this feature does not preclude stem-anseriform affinities for *Asteriornis*; although common to all

393 members of Anatidae, a recessus conicalis is absent in Anhimidae and *Nettapterornis* (Olson, 1999)  
394 and is only shallow in *Anseranas* (the extant sister group to Anatidae) and in the fossil pan-  
395 anseriforms *Presbyornis* and *Conficto* (Ericson, 1997; Tambussi et al., 2019). If an enlarged  
396 retroarticular process were present in *Asteriornis*, it may therefore be unlikely for it to have exhibited  
397 the extremely mediolaterally compressed, ‘blade-like’ morphology common to *Anseranas* and  
398 Anatidae (Fig. 3b,c), all of which also possess some form of recessus conicalis (Olson & Feduccia,  
399 1980; Baumel & Witmer, 1993; Olson, 1999; Zelenkov & Stidham, 2018). We propose that the  
400 presence of a recessus conicalis and an anatid-like retroarticular process may be developmentally  
401 correlated, with the development of a recessus conicalis potentially constraining the mediolateral  
402 width of the retroarticular process by reducing the mediolateral extent of the caudal part of the  
403 mandible where the retroarticular attaches.

404 *Extant non-galloanseran Neornithes*

405 The caudal region of the mandibles of the palaeognaths *Struthio* and *Eudromia* (Fig. 4h,i) are  
406 morphologically dissimilar to that of *Asteriornis*. In both palaeognath taxa, the medial process is  
407 rostrocaudally broad and dorsoventrally shallow, especially in *Eudromia*, contrasting with the medial  
408 processes of *Asteriornis* and other extant galloanserans which are more pointed and dorsoventrally  
409 deep. The medial process of the palaeognaths is only very slightly dorsally deflected, as opposed to  
410 the shallow but obvious dorsal deflection of the process in *Asteriornis*. The lateral process is a small  
411 and indistinct dorsally-positioned ridge in *Struthio* and completely absent in *Eudromia*, contrasting  
412 with the distinct lateral process of *Asteriornis*. When the retroarticular region is digitally removed, the  
413 cross section of the remaining portion of the palaeognath caudal mandible is very different from the  
414 preserved caudal end of the *Asteriornis* mandible; the dorsal surface is prominently concave in both  
415 palaeognath taxa, while the exposed region is bulbous in *Struthio* (Fig. 4h) and uniformly thin  
416 dorsoventrally in *Eudromia* (Fig. 4i), in contrast to the broadly triangular cross-section of the articular  
417 region of *Asteriornis*. Even accounting for the uncertain presence of a retroarticular process, the  
418 morphology of the preserved parts of the caudal end of the mandible in *Asteriornis* are substantially  
419 more similar to those of galloanserans than those of palaeognaths. As such, the morphology of the

420 caudal portion of the mandible casts further doubt on the total-group palaeognath affinities recovered  
421 for *Asteriornis* in some analyses (Torres et al., 2021; Benito et al., 2022b).

422 The preserved caudal end of the mandible of *Asteriornis* bears little morphological  
423 resemblance to those of the sampled neoavians, regardless of the presence of enlarged retroarticular  
424 processes. In *Puffinus puffinus* (Fig. 4k), which does not possess an enlarged retroarticular process,  
425 the medial process is angled so that the tip is directed caudally, extending to the same caudal position  
426 as the main body of the articular, and the caudal end of the mandible is much deeper dorsoventrally  
427 than that of *Asteriornis*. The lateral process is small and indistinct, presenting as only a slightly raised  
428 ridge on the lateral surface, and the medial process is proportionally small compared with that of the  
429 galloanserans examined. The dorsoventral depth of the articular region, the proportions of the medial  
430 and lateral processes, and the medially curved midline of the ramus at the caudal end yield a  
431 morphology of the caudal extremity of the mandible distinctly unlike that of *Asteriornis*. In  
432 *Phoenicopterus* (Fig. 4j), a neoavian with a retroarticular process that has been considered  
433 morphologically comparable to that of galloanserans (Ericson, 1996, 1997), the articular region is  
434 extremely deep dorsoventrally and narrow mediolaterally, with a medial process that is small and  
435 steeply angled dorsally. The medial process is pointed, with a sharp rostrally pointed hook, and the  
436 lateral process is completely absent. The retroarticular itself exhibits a unique morphology with a  
437 distinct dorsal process at its base and a slightly flared, rounded tip (Fig. 3i) unlike the sharp hooks  
438 seen in anatids (Fig. 3b,c).

439

440 *Other fossil birds*

441 The fact that the possible presence of an enlarged retroarticular process cannot be excluded in  
442 *Asteriornis* is particularly significant in the context of comparisons with other putative total-group  
443 galloanserans, notably *Vegavis* and Pelagornithidae. The mandible of *Vegavis* is known from a partial  
444 fragment of the postdentary complex, from which the absence of a large retroarticular has been  
445 inferred (Clarke et al., 2016; Mayr et al., 2018). Similarly, an enlarged retroarticular is known to be

446 absent in pelagornithids (Bourdon, 2005; Mayr & Rubilar-Rogers, 2010). The galloanseran affinities  
447 of pelagornithids have recently been called into question; some characteristics thought to unite them  
448 with Galloanserae, notably a bicondylar quadrate-mandibular articulation and the morphology of the  
449 pterygoid, have instead been reinterpreted as possible crown bird plesiomorphies (Mayr et al., 2018;  
450 Tambussi et al., 2019; Benito et al., 2022b), and the morphology of the articular end of the  
451 pelagornithid mandible was considered to be very similar to that seen in the crownward stem bird  
452 clade Ichthyornithes (Mayr et al., 2021). By contrast, the lack of an enlarged retroarticular in non-  
453 neornithine members of Ornithurae such as *Ichthyornis* (Clarke, 2004) and Hesperornithes (Martin &  
454 Naples, 2008) supports the interpretation of this feature as a galloanseran synapomorphy. As  
455 discussed above, all extant galloanserans exhibit large and distinct retroarticular processes, as do  
456 known fossil pan-anseriforms such as *Anachronornis*, *Nettapterornis*, *Conflictornis* and *Presbyornis*  
457 (Livezey, 1997; Olson, 1999; Tambussi et al., 2019; Houde et al., 2023), further suggesting that this  
458 morphology may have been present early in galloanseran evolutionary history. The confirmed absence  
459 of a retroarticular process in pelagornithids and *Vegavis*, in contrast to its unknown state in  
460 *Asteriornis*, is therefore worth considering in relation to the phylogenetic placement of these taxa and  
461 the distribution of this character through galloanseran evolutionary history.

462

### 463 **Conclusions**

464 It is now understood that no retroarticular process is preserved in the holotype of *Asteriornis*;  
465 however, we cannot exclude the possibility of this feature having originally been present. The damage  
466 to the caudal ends of the mandibular rami of this specimen is extensive enough to have obscured any  
467 evidence that could unambiguously indicate the presence or absence of a retroarticular process. The  
468 portions of the mandible to which a possible retroarticular process would attach, based on  
469 comparisons with the mandibles of extant birds, are clearly missing from both mandibular rami, and  
470 thus it is currently impossible to exclude the possibility of a retroarticular process having originally  
471 been present in *Asteriornis*. This is in contrast to other putative total-group galloanserans for which  
472 the absence of a retroarticular process is known, including the only other well-established Mesozoic

473 neornithine, *Vegavis* (Clarke et al., 2016), and the enigmatic extinct clade Pelagornithidae (Mayr &  
474 Rubilar-Rogers, 2010).

475 The position of *Asteriornis* within total-group Galloanserae is supported by our updated  
476 phylogenetic analyses reflecting the now unknown presence and morphology of the retroarticular  
477 process. Despite the uncertainty regarding this key galloanseran synapomorphy, other morphological  
478 features of the skull, and particularly the quadrate, continue to support galloanseran affinities for  
479 *Asteriornis*. This position appears to be further supported by novel observations of morphological  
480 similarities between the preserved caudal ends of the mandible of *Asteriornis* and those of modern  
481 galloanseran specimens where the retroarticular region was artificially removed. Most notable is the  
482 strong resemblance between the caudal part of the mandible of *Asteriornis* and the homologous region  
483 of megapodes and anhimids, the extant sister taxa to the rest of galliforms and anseriforms,  
484 respectively. This observation is consistent with the hypothesis of *Asteriornis* as a total-group  
485 galloanseran, phylogenetically proximal to the divergence between the galliform and anseriform  
486 lineages. Overall, this work revises our understanding of the mandibular morphology and  
487 phylogenetic position of *Asteriornis*, one of the oldest known neornithine birds and a critical datapoint  
488 in our evolving understanding of crown bird origins.

489

## 490 **Acknowledgements**

491 We would like to thank M. Dickson for sharing details about the phylogenetic analyses run by Houde  
492 et al. (2023). J.B. and D.J.F. were funded by UKRI grant MR/S032177/1 to D.J.F. For the purpose of  
493 open access, the authors have applied a Creative Commons Attribution (CC-BY) licence to any  
494 Author Accepted Manuscript version arising.

495

## 496 **References**

497 Barido-Sottani, J., Aguirre-Fernández, G., Hopkins, M. J., Stadler, T., & Warnock, R. (2019).

498 Ignoring stratigraphic age uncertainty leads to erroneous estimates of species divergence  
499 times under the fossilized birth–death process. *Proceedings of the Royal Society B*,  
500 286(1902), 20190685.

501 Baumel, J., & Witmer, L. (1993). Osteologia. 45–132. In *Handbook of avian anatomy: Nomina*  
502 *anatomica avium. Second edition. Publications of the Nuttall Ornithological Club*,  
503 *Cambridge, MA*.

504 Beecher, W. J. (1951). Adaptations for food-getting in the American blackbirds. *The Auk*, 68(4), 411–  
505 440.

506 Benito, J., Kuo, P.-C., Widrig, K. E., Jagt, J. W. M., & Field, D. J. (2022a). Cretaceous ornithurine  
507 supports a neognathous crown bird ancestor. *Nature*, 612(7938), 100–105.

508 Benito, J., Chen, A., Wilson, L. E., Bhullar, B.-A. S., Burnham, D., & Field, D. J. (2022b). Forty new  
509 specimens of *Ichthyornis* provide unprecedented insight into the postcranial morphology of  
510 crownward stem group birds. *PeerJ*, 10, e13919.

511 Benton, M. J., & Donoghue, P. C. (2007). Paleontological evidence to date the tree of life. *Molecular*  
512 *Biology and Evolution*, 24(1), 26–53.

513 Bock, W. J. (1964). Kinetics of the avian skull. *Journal of Morphology*, 114(1), 1–41.

514 Bourdon, E. (2005). Osteological evidence for sister group relationship between pseudo-toothed birds  
515 (Aves: Odontopterygiformes) and waterfowls (Anseriformes). *Naturwissenschaften*, 92(12),  
516 586–591.

517 Bourdon, E., Amaghzaz, M., & Bouya, B. (2010). Pseudotoothed birds (Aves, Odontopterygiformes)  
518 from the early Tertiary of Morocco. *American Museum Novitates*, 2010(3704), 1–71.

519 Clarke, J. A. (2004). Morphology, phylogenetic taxonomy, and systematics of *Ichthyornis* and  
520 *Apatornis* (Avialae: Ornithurae). *Bulletin of the American museum of natural history*,  
521 2004(286), 1–179.

522 Clarke, J. A., Chatterjee, S., Li, Z., Riede, T., Agnolin, F., Goller, F., Isasi, M. P., Martinioni, D. R.,  
523 Mussel, F. J., & Novas, F. E. (2016). Fossil evidence of the avian vocal organ from the  
524 Mesozoic. *Nature*, 538(7626), 502–505.

525 Clarke, J. A., Tambussi, C. P., Noriega, J. I., Erickson, G. M., & Ketcham, R. A. (2005). Definitive  
526 fossil evidence for the extant avian radiation in the Cretaceous. *Nature*, 433(7023), 305-308.

527 Collinson, M. E., Adams, N. F., Manchester, S. R., Stull, G. W., Herrera, F., Smith, S. Y., Andrew,  
528 M. J., Kenrick, P., & Sykes, D. (2016). X-ray micro-computed tomography (micro-CT) of  
529 pyrite-permineralized fruits and seeds from the London Clay Formation (Ypresian) conserved  
530 in silicone oil: a critical evaluation. *Botany*, 94(9), 697-711.

531 Cracraft, J. (2001). Avian evolution, Gondwana biogeography and the Cretaceous–Tertiary mass  
532 extinction event. *Proceedings of the Royal Society of London. Series B: Biological Sciences*,  
533 268(1466), 459-469.

534 Cracraft, J., Clarke, J., Gauthier, J., & Gall, L. (2001). New perspectives on the origin and early  
535 evolution of birds. *Special Publication Peabody Museum of Natural History*, 143-156.

536 Cracraft, J., & Mindell, D. P. (1989). The early history of modern birds: a comparison of molecular  
537 and morphological evidence.

538 Elzanowski, A., & Boles, W. E. (2012). Australia's oldest Anseriform fossil: a quadrate from the  
539 Early Eocene Tingamarra Fauna. *Palaeontology*, 55(4), 903-911.

540 Elzanowski, A., & Stidham, T. A. (2010). Morphology of the quadrate in the Eocene anseriform  
541 *Presbyornis* and extant galloanserine birds. *Journal of Morphology*, 271(3), 305-323.

542 Elzanowski, A., & Stidham, T. A. (2011). A galloanserine quadrate from the Late Cretaceous Lance  
543 Formation of Wyoming. *The Auk*, 128(1), 138-145.

544 Ericson, P. G. (1996). The skeletal evidence for a sister-group relationship of anseriform and  
545 galliform birds: a critical evaluation. *Journal of Avian Biology*, 195-202.

546 Ericson, P. G. (1997). Systematic relationships of the palaeogene family Presbyornithidae (Aves:  
547 Anseriformes). *Zoological Journal of the Linnean Society*, 121(4), 429-483.

548 Ericson, P. G., Anderson, C. L., Britton, T., Elzanowski, A., Johansson, U. S., Källersjö, M., Ohlson,  
549 J. I., Parsons, T. J., Zuccon, D., & Mayr, G. (2006). Diversification of Neoaves: integration of  
550 molecular sequence data and fossils. *Biology letters*, 2(4), 543-547.

551 Feduccia, A. (1999). *The origin and evolution of birds*. Yale University Press.

552 Field, D. J., Benito, J., Chen, A., Jagt, J. W. M., & Ksepka, D. T. (2020). Late Cretaceous neornithine  
553 from Europe illuminates the origins of crown birds. *Nature*, 579(7799), 397-401.

554 Field, D.J., Berv, J.S., Hsiang, A.Y., Lanfear, R., Landis, M.J., & Dornburg, A. (2020). Timing the  
555 extant avian radiation: The rise of modern birds, and the importance of modeling molecular  
556 rate variation. In *Pennaraptoran theropod dinosaurs: Past progress and new frontiers* (Pittman,  
557 M. & Xing, X. Eds.). *Bulletin of the American Museum of Natural History* 440: 159-181.

558 Garrod, A. H. (1873). On certain muscles of the thigh of birds and on their value in classification.

559 Goloboff, P. A., & Catalano, S. A. (2016). TNT version 1.5, including a full implementation of  
560 phylogenetic morphometrics. *Cladistics*, 32(3), 221-238.

561 Gonzalez, J., Düttmann, H., & Wink, M. (2009). Phylogenetic relationships based on two  
562 mitochondrial genes and hybridization patterns in Anatidae. *Journal of Zoology*, 279(3), 310-  
563 318.

564 Hackett, S. J., Kimball, R. T., Reddy, S., Bowie, R. C., Braun, E. L., Braun, M. J., Chojnowski, J. L.,  
565 Cox, W. A., Han, K.-L., & Harshman, J. (2008). A phylogenomic study of birds reveals their  
566 evolutionary history. *Science*, 320(5884), 1763-1768.

567 Harris, R. B., Birks, S. M., & Leaché, A. D. (2014). Incubator birds: biogeographical origins and  
568 evolution of underground nesting in megapodes (Galliformes: Megapodiidae). *Journal of  
569 Biogeography*, 41(11), 2045-2056.

570 Hospitaleche, C. A., & Worthy, T. H. (2021). New data on the Vegavis iaai holotype from the  
571 Maastrichtian of Antarctica. *Cretaceous Research*, 124, 104818.

572 Houde, P., Dickson, M., & Camarena, D. (2023). Basal Anseriformes from the Early Paleogene of  
573 North America and Europe. *Diversity*, 15(2), 233.

574 Jarvis, E. D., Mirarab, S., Aberer, A. J., Li, B., Houde, P., Li, C., Ho, S. Y., Faircloth, B. C., Nabholz,  
575 B., & Howard, J. T. (2014). Whole-genome analyses resolve early branches in the tree of life  
576 of modern birds. *Science*, 346(6215), 1320-1331.

577 Kimball, R. T., Hosner, P. A., & Braun, E. L. (2021). A phylogenomic supermatrix of Galliformes  
578 (Landfowl) reveals biased branch lengths. *Molecular Phylogenetics and Evolution*, 158,  
579 107091.

580 Kimball, R. T., Oliveros, C. H., Wang, N., White, N. D., Barker, F. K., Field, D. J., Ksepka, D. T.,  
581 Chesser, R. T., Moyle, R. G., & Braun, M. J. (2019). A phylogenomic supertree of birds.  
582 *Diversity*, 11(7), 109.

583 Ksepka, D., & Clarke, J. (2015). Phylogenetically vetted and stratigraphically constrained fossil  
584 calibrations within Aves. *Palaeontologia Electronica*, 18(1), 1-25.

585 Kuhl, H., Frankl-Vilches, C., Bakker, A., Mayr, G., Nikolaus, G., Boerno, S. T., Klages, S.,  
586 Timmermann, B., & Gahr, M. (2021). An unbiased molecular approach using 3'-UTRs  
587 resolves the avian family-level tree of life. *Molecular Biology and Evolution*, 38(1), 108-127.

588 Kuo, P.-C., Benson, R. B., & Field, D. J. (2023). The influence of fossils in macroevolutionary  
589 analyses of 3D geometric morphometric data: A case study of galloanseran quadrates. *Journal  
590 of Morphology*, 284(6), e21594.

591 Kuramoto, T., Nishihara, H., Watanabe, M., & Okada, N. (2015). Determining the position of storks  
592 on the phylogenetic tree of waterbirds by retroposon insertion analysis. *Genome biology and  
593 evolution*, 7(12), 3180-3189.

594 Livezey, B., & Zusi, R. (2006). Higher-Order Phylogeny of Modern Birds (Theropoda, Aves:  
595 Neornithes) Based on Comparative Anatomy. 1, Methods and Characters. Carnegie Museum  
596 of Natural History 37, 1-556. In.

597 Livezey, B. C. (1997). A phylogenetic analysis of basal Anseriformes, the fossil Presbyornis, and the  
598 interordinal relationships of waterfowl. *Zoological Journal of the Linnean Society*, 121(4),  
599 361-428.

600 Longrich, N. R., Tokaryk, T., & Field, D. J. (2011). Mass extinction of birds at the Cretaceous–  
601 Paleogene (K–Pg) boundary. *Proceedings of the National Academy of Sciences*, 108(37),  
602 15253-15257.

603 Martin, L. D., & Naples, V. L. (2008). Mandibular kinesis in Hesperornis. *Oryctos*, 7, 61-65.

604 Mayr, G. (2005). A new Eocene Chascacocolius-like mousebird (Aves: Coliiformes) with a  
605 remarkable gaping adaptation. *Organisms Diversity & Evolution*, 5(3), 167-171.

606 Mayr, G. (2008). The higher-level phylogeny of birds-when morphology, molecules, and fossils  
607 coincide. *Oryctos*, 7, 67-73.

608 Mayr, G. (2011). Metaves, Mirandornithes, Strisores and other novelties—a critical review of the  
609 higher-level phylogeny of neornithine birds. *Journal of Zoological Systematics and*  
610 *Evolutionary Research*, 49(1), 58-76.

611 Mayr, G. (2013). Late Oligocene mousebird converges on parrots in skull morphology. *Ibis*, 155(2),  
612 384-396.

613 Mayr, G. (2016). *Avian evolution: the fossil record of birds and its paleobiological significance*. John  
614 Wiley & Sons.

615 Mayr, G. (2022a). Basic Terminology and the Broader Phylogenetic and Geological Framework. In  
616 *Paleogene Fossil Birds* (pp. 3-27). Springer.

617 Mayr, G. (2022b). Pelagornithidae, Gastornithidae, and Crown Group Galloanseres. In *Paleogene*  
618 *Fossil Birds* (pp. 43-72). Springer.

619 Mayr, G., & Clarke, J. (2003). The deep divergences of neornithine birds: a phylogenetic analysis of  
620 morphological characters. *Cladistics*, 19(6), 527-553.

621 Mayr, G., De Pietri, V. L., Love, L., Mannering, A., & Scofield, R. P. (2021). Oldest, smallest and  
622 phylogenetically most basal pelagornithid, from the early Paleocene of New Zealand, sheds  
623 light on the evolutionary history of the largest flying birds. *Papers in Palaeontology*, 7(1),  
624 217-233.

625 Mayr, G., De Pietri, V. L., Scofield, R. P., & Worthy, T. H. (2018). On the taxonomic composition  
626 and phylogenetic affinities of the recently proposed clade Vegaviidae Agnolín et al., 2017—  
627 neornithine birds from the Upper Cretaceous of the Southern Hemisphere. *Cretaceous*  
628 *Research*, 86, 178-185.

629 Mayr, G., & Rubilar-Rogers, D. (2010). Osteology of a new giant bony-toothed bird from the  
630 Miocene of Chile, with a revision of the taxonomy of Neogene Pelagornithidae. *Journal of*  
631 *Vertebrate Paleontology*, 30(5), 1313-1330.

632 Miller, M. A., Pfeiffer, W., & Schwartz, T. (2010). Creating the CIPRES Science Gateway for  
633 inference of large phylogenetic trees. 2010 gateway computing environments workshop  
634 (GCE),

635 Mindell, D.P., (2020). Galloanserae, K. De Queiroz, P.D. Cantino, J. Gauthier (Eds.), *Phylogenoms: a*  
636 *Companion to the PhyloCode*, CRC Press, Taylor & Francis Group, Boca Raton, pp. 1255-  
637 1257

638 Musser, G. and J. A. Clarke. 2022. A new Paleogene fossil and a new dataset for waterfowl (Aves:  
639 Anseriformes) clarify phylogeny, ecological evolution, and avian evolution at the K-Pg  
640 Boundary.

641 Olson, S. L. (1999). The anseriform relationships of Anatalavis Olson and Parris (Anseranatidae),  
642 with a new species from the Lower Eocene London Clay. *Avian paleontology at the close of*  
643 *the 20th century*.

644 Olson, S. L., & Feduccia, A. (1980). Presbyornis and the origin of the Anseriformes (Aves:  
645 Charadriomorphae).

646 Previatto, D. M. (2012). Osteologia craniana da família Anhimidae (Aves: Anseriformes).

647 Prum, R. O., Berv, J. S., Dornburg, A., Field, D. J., Townsend, J. P., Lemmon, E. M., & Lemmon, A.  
648 R. (2015). A comprehensive phylogeny of birds (Aves) using targeted next-generation DNA  
649 sequencing. *Nature*, 526(7574), 569-573.

650 Püschel, H. P., O'Reilly, J. E., Pisani, D., & Donoghue, P. C. (2020). The impact of fossil stratigraphic  
651 ranges on tip-calibration, and the accuracy and precision of divergence time estimates.  
652 *Palaeontology*, 63(1), 67-83.

653 Reddy, S., Kimball, R. T., Pandey, A., Hosner, P. A., Braun, M. J., Hackett, S. J., Han, K.-L.,  
654 Harshman, J., Huddleston, C. J., & Kingston, S. (2017). Why do phylogenomic data sets yield  
655 conflicting trees? Data type influences the avian tree of life more than taxon sampling.  
656 *Systematic Biology*, 66(5), 857-879.

657 Roberts, E. M., O'Connor, P. M., Clarke, J. A., Slotnick, S. P., Placzek, C. J., Tobin, T. S.,  
658 Hannaford, C., Orr, T., Jinnah, Z. A., & Claeson, K. M. (2023). New age constraints support a  
659 K/Pg boundary interval on Vega Island, Antarctica: Implications for latest Cretaceous  
660 vertebrates and paleoenvironments. *Bulletin*, 135(3-4), 867-885.

661 Ronquist, F., Teslenko, M., Van Der Mark, P., Ayres, D. L., Darling, A., Höhna, S., Larget, B., Liu,  
662 L., Suchard, M. A., & Huelsenbeck, J. P. (2012). MrBayes 3.2: efficient Bayesian  
663 phylogenetic inference and model choice across a large model space. *Systematic Biology*,  
664 61(3), 539-542.

665 Sibley, C. G., & Ahlquist, J. E. (1990). *Phylogeny and classification of birds: a study in molecular*  
666 *evolution* (Vol. 10). JSTOR.

667 Simmons, M. P., Springer, M. S., & Gatesy, J. (2022). Gene-tree misrooting drives conflicts in  
668 phylogenomic coalescent analyses of palaeognath birds. *Molecular Phylogenetics and*  
669 *Evolution*, 167, 107344.

670 Tambussi, C. P., Degrange, F. J., De Mendoza, R. S., Sferco, E., & Santillana, S. (2019). A stem  
671 anseriform from the early Palaeocene of Antarctica provides new key evidence in the early  
672 evolution of waterfowl. *Zoological Journal of the Linnean Society*, 186(3), 673-700.

673 Torres, C. R., Norell, M. A., & Clarke, J. A. (2021). Bird neurocranial and body mass evolution  
674 across the end-Cretaceous mass extinction: The avian brain shape left other dinosaurs behind.  
675 *Science Advances*, 7(31), eabg7099.

676 Vanden Berge, J., & Zweers, G. (1993). Myologia. 189-250. In *Handbook of avian anatomy: Nomina*  
677 *anatomica avium. Second edition. Publications of the Nuttall Ornithological Club*,  
678 *Cambridge, MA*

679 Vellekoop, J., Kaskes, P., Sinnesael, M., Huygh, J., Déhais, T., Jagt, J. W., Speijer, R. P., & Claeys, P.  
680 (2022). A new age model and chemostratigraphic framework for the Maastrichtian type area  
681 (southeastern Netherlands, northeastern Belgium). *Newsletters on Stratigraphy*.

682 Widrig, K., & Field, D.J. (2022). The Evolution and Fossil Record of Palaeognathous Birds  
683 (Neornithes: Palaeognathae). *Diversity* 14(2):105. <https://doi.org/10.3390/d14020105>

684 Worthy, T. H., Degrange, F. J., Handley, W. D., & Lee, M. S. (2017). The evolution of giant flightless  
685 birds and novel phylogenetic relationships for extinct fowl (Aves, Galloanseres). *Royal*  
686 *Society open science*, 4(10), 170975.

687 Zelenkov, N., & Stidham, T. A. (2018). Possible filter-feeding in the extinct Presbyornis and the  
688 evolution of Anseriformes (Aves).

689 Zhang, C., Stadler, T., Klopstein, S., Heath, T. A., & Ronquist, F. (2016). Total-evidence dating  
690 under the fossilized birth–death process. *Systematic Biology*, 65(2), 228-249.

691 Zusi, R. L. (1967). The role of the depressor mandibulae muscle in kinesis of the avian skull.  
692 *Proceedings of the United States National Museum*.

693 Zweers, G., & Berge, J. V. (1996). Evolutionary transitions in the trophic system of the wader-  
694 waterfowl complex. *Netherlands Journal of Zoology*, 47(3), 255-287.

695

696 **Figure Captions**

697 **Figure 1. Mandible of *Asteriornis* holotype, as preserved.** Whole mandible shown in dorsal,  
698 ventral, left and right lateral views. Scale bar equals 10mm.

699 **Figure 2. Caudal ends of the *Asteriornis* mandible.** A) Whole mandible shown in dorsal view (with  
700 respect to mandibular symphysis). B,C) Caudal sections of right and left ramus shown separately in  
701 dorsal, ventral, medial, lateral and caudal views. B) Left ramus: dorsal surface left in medial view,  
702 right in lateral view. C) Right ramus: dorsal surface right in medial view, left in lateral view. Scale bar  
703 equals 10mm.

704 **Figure 3. Caudal ends of the left mandibular ramus of a selection of extant taxa with  
705 retroarticular regions rendered transparent.** Caudal ends of left mandibles in dorsal, ventral,  
706 medial and lateral views. Dorsal surface left in medial view and right in lateral view. Scale bar equals  
707 10mm.

708 **Figure 4. Caudal ends of the left mandibular ramus of *Asteriornis* and selected extant taxa.** Extant  
709 taxa shown with retroarticular/caudal end of the mandible present and digitally removed. Positioned as  
710 viewed in the plane of exposure on the fossil block. Major region of broken/missing material of  
711 *Asteriornis* highlighted in red. Scale bar equals 5mm.

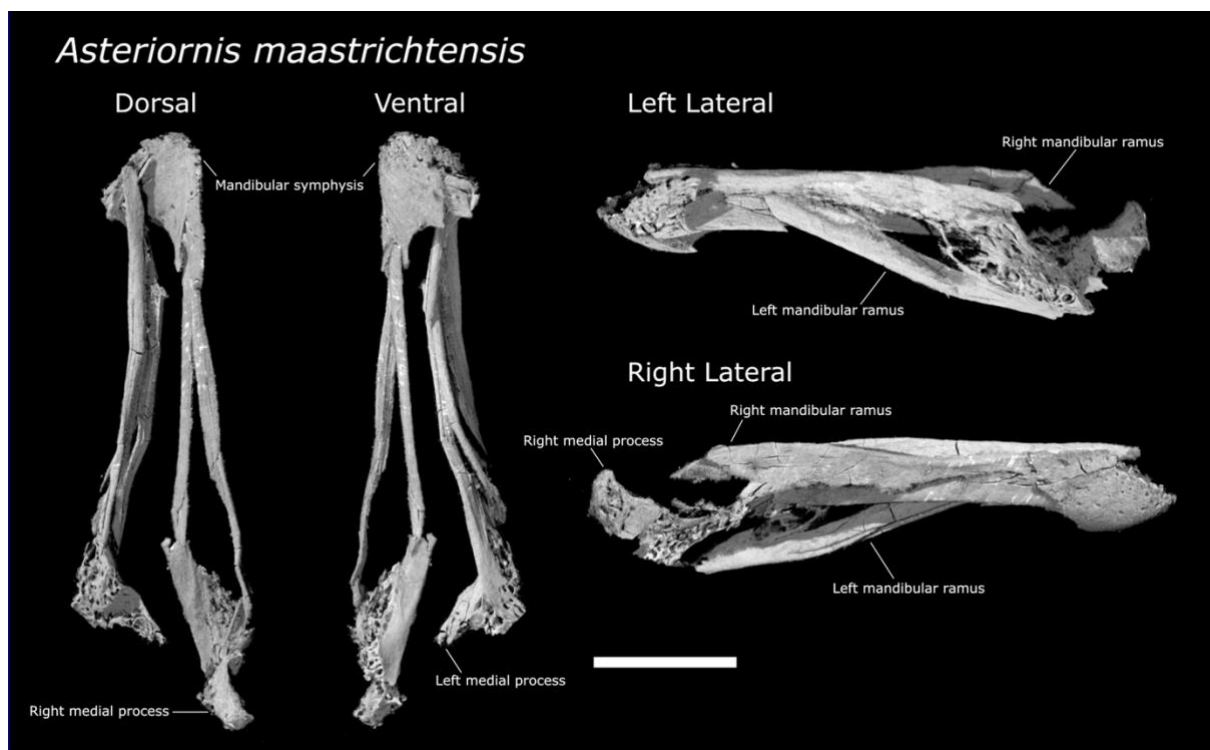
712 **Figure 5. Cladogram showing recovered phylogenetic positions of *Asteriornis* and *Vegavis* under**  
713 **parsimony analyses.** The presence, absence and uncertain presence of retroarticular processes is

714 indicated, with silhouettes of a representative retroarticular morphology illustrated for those clades for

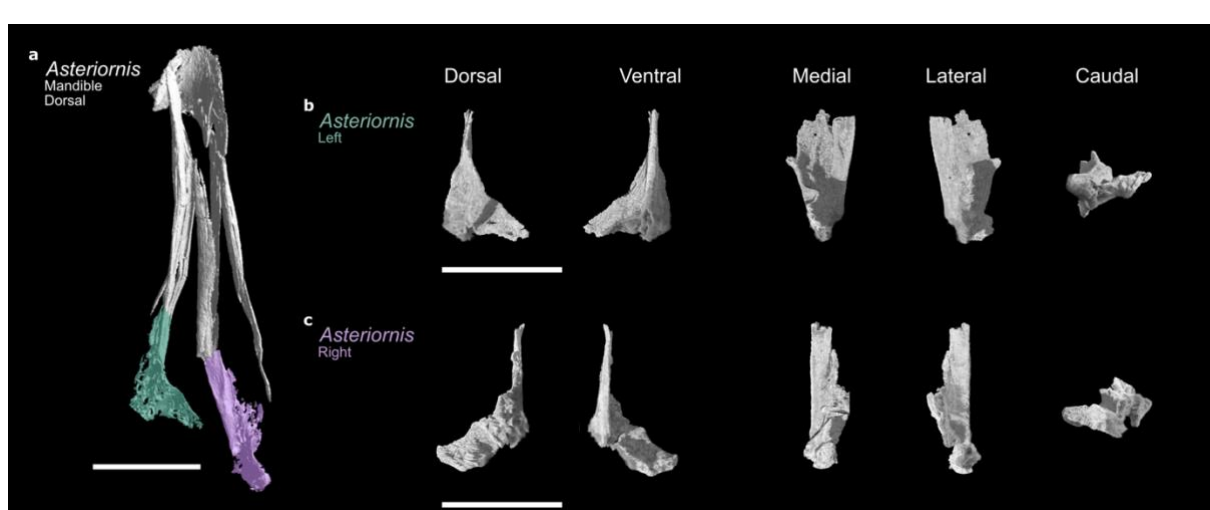
715 which retroarticular processes are known.

716

717 **Fig. 1**

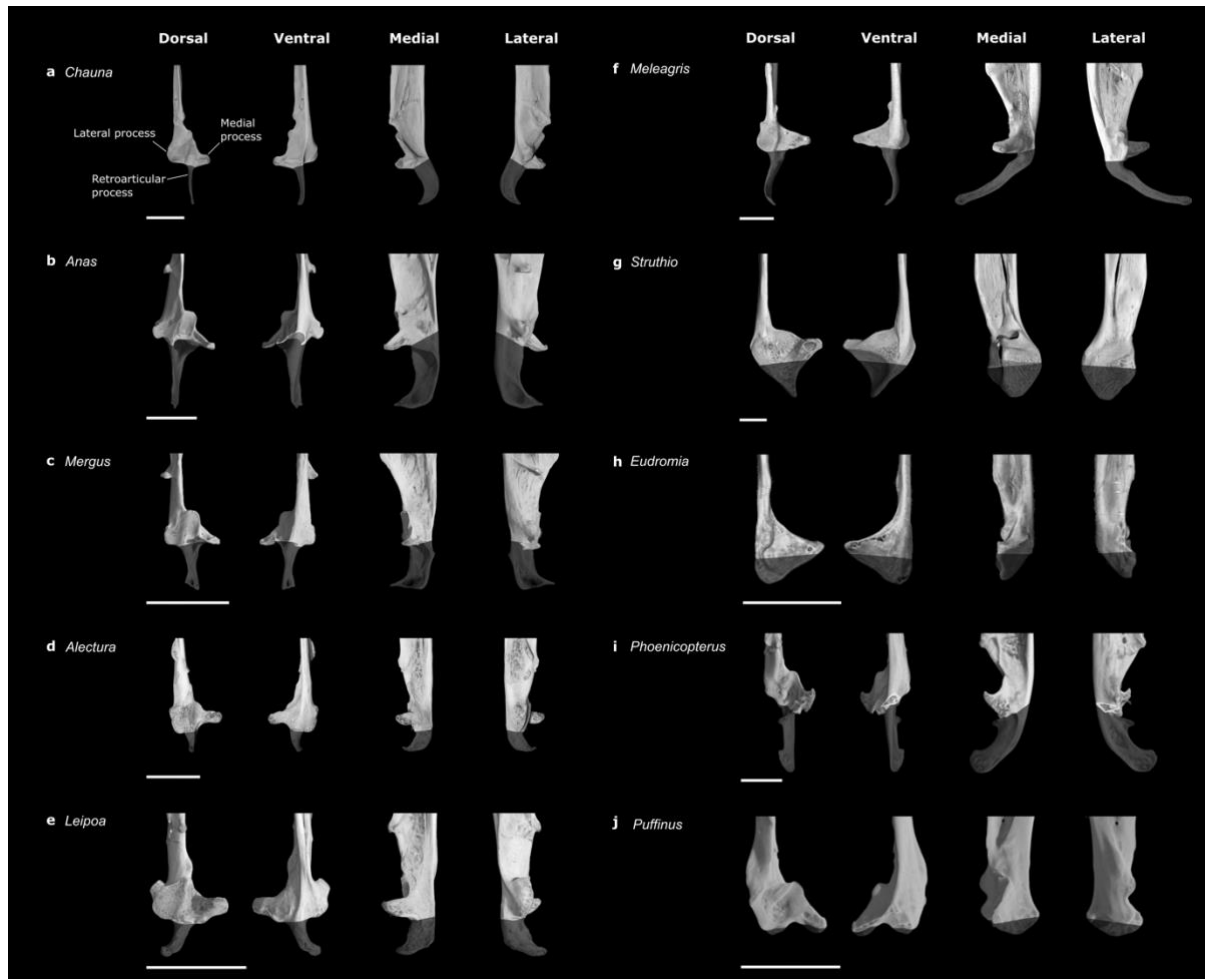


719



720

721 **Fig. 3.**



722

723

724

725

726

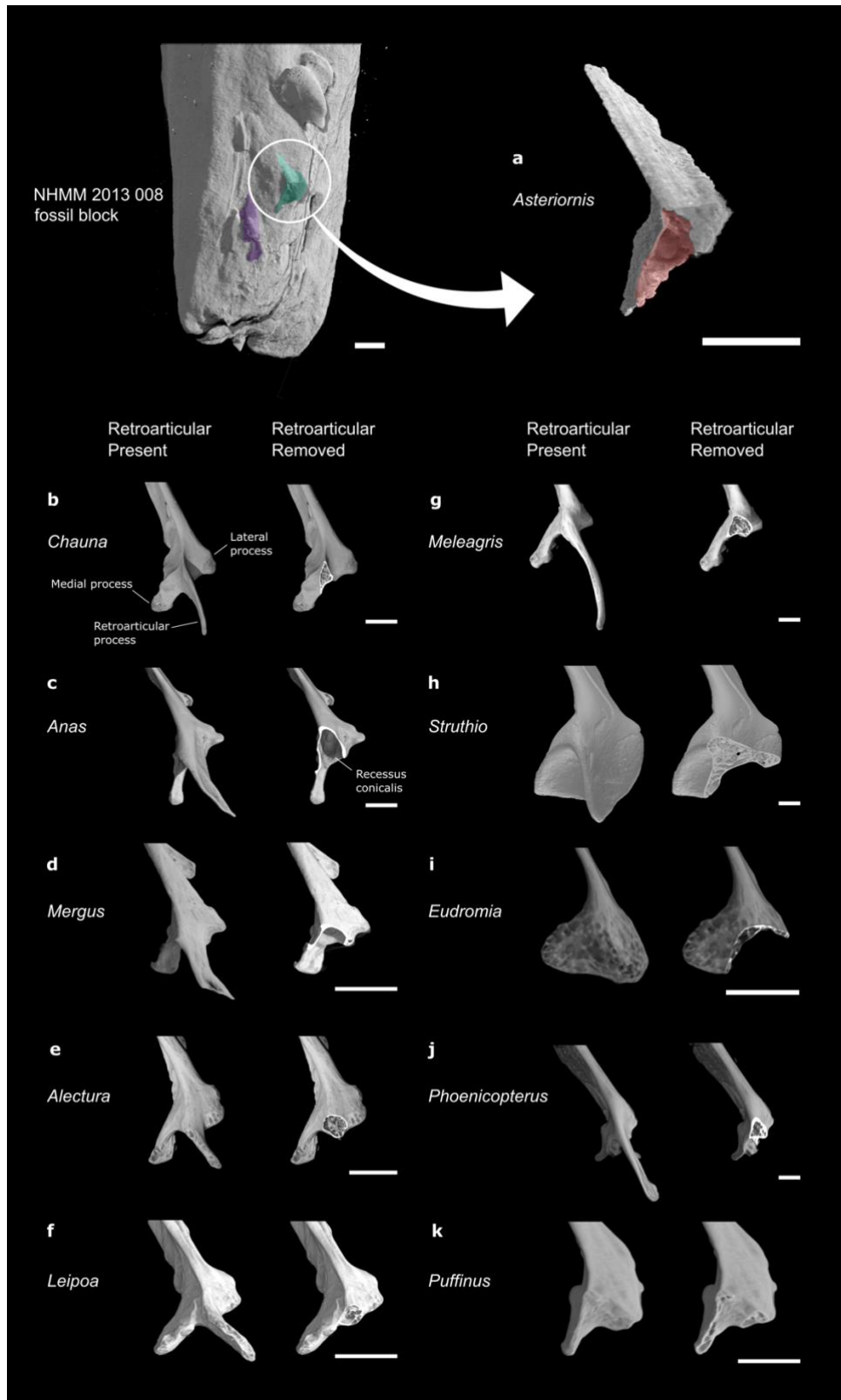
727

728

729

730

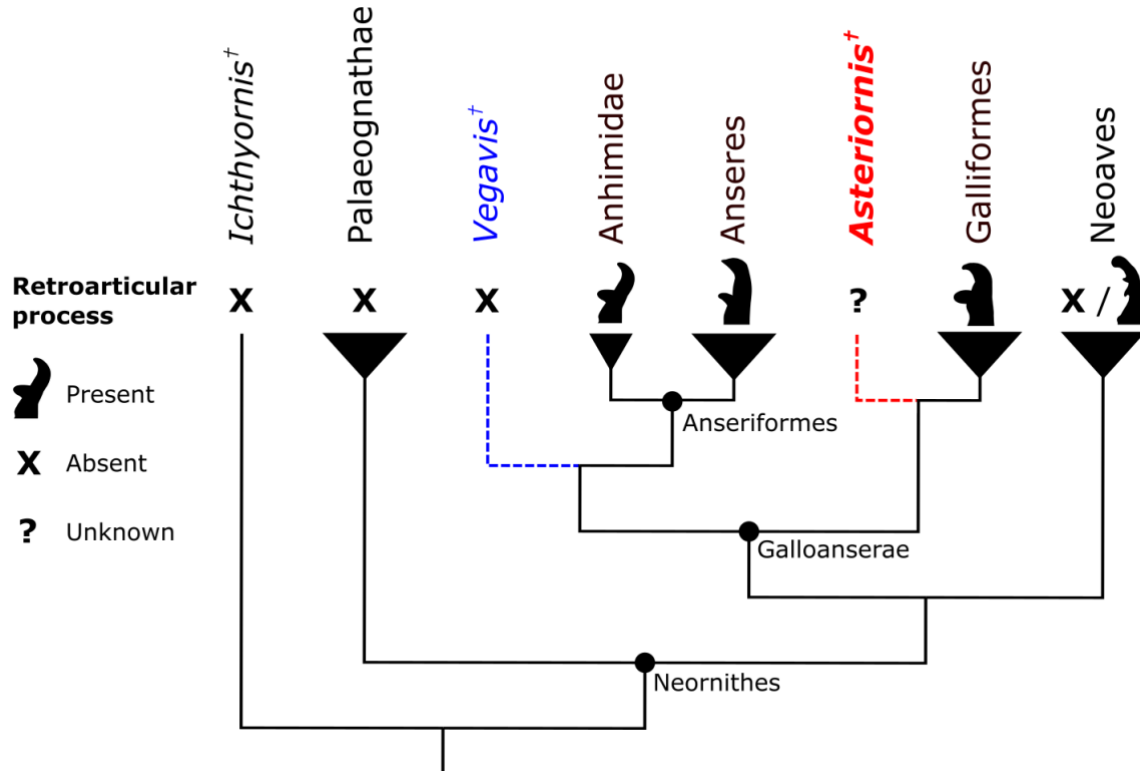
731 **Fig. 4**



732

733

734 **Fig. 5**



735